Journal of Photochemistry and Photobiology A: Chemistry 212 (2010) 129–134

Contents lists available at ScienceDirect

Journal of Photochemistry and Photobiology A: Chemistry

journal homepage: www.elsevier.com/locate/jphotochem

Synthesis and time-resolved fluorescence study of porphyrin-functionalized gold nanoparticles

Anne Kotiaho[a,*], Riikka Lahtinen[a], Alexander Efimov[a], Heli Lehtivuori[a], Nikolai V. Tkachenko[a], Tomi Kanerva[b], Helge Lemmetyinen[a]

[a] Department of Chemistry and Bioengineering, Tampere University of Technology, P.O. Box 541, 33101 Tampere, Finland
[b] Department of Materials Science, Tampere University of Technology, P.O. Box 589, 33101 Tampere, Finland

ARTICLE INFO

Article history:
Received 24 February 2010
Received in revised form 22 March 2010
Accepted 4 April 2010
Available online 10 April 2010

Keywords:
Porphyrin
Gold nanoparticles
Fluorescence lifetime
Energy transfer

ABSTRACT

Free-base porphyrins with two thioacetate terminated linkers in different positions on the porphyrin molecule were synthesized and attached to tetraoctylammonium bromide (TOABr) stabilized gold nanoparticles with a core diameter of 5 nm. The different positions of the linkers affect the stability of the functionalized gold nanoparticles and have an effect on the packing density of the molecules on the nanoparticle surface. However, the intended control of the orientation of the porphyrin molecules relative to the gold nanoparticle surface is not well achieved with the chosen linkers. Fluorescence of the porphyrins is observed to be strongly quenched after the attachment to the nanoparticles. Fluorescence lifetimes of the porphyrin-functionalized gold nanoparticles were determined with the up-conversion method to be very short, 3–5 ps. The short fluorescence lifetimes indicate efficient energy transfer to the gold cores.

1. Introduction

Porphyrins on gold nanoparticle surfaces have applications in photocurrent generation [1], photocatalysis [2] and sensors [3]. The operation of porphyrin-functionalized gold nanoparticles depends on how the systems are assembled. Porphyrins have been attached to gold nanoparticle surfaces in perpendicular (one linker) [4] or parallel (four linkers) [3,5,6] orientations relative to the gold surface. The advantage of the use of multiple binding sites is to achieve a better control on the orientation of porphyrin on the gold core. Also, in the case of self-assembled monolayers on flat gold films, the packing of porphyrins is affected by the nature of the linkers [7,8]. Understanding and controlling the factors affecting the interaction between chromophores and metal nanoparticles is essential in designing effective applications.

The most frequently reported photoinduced process in chromophore-functionalized gold nanoparticles is energy transfer from a photoexcited chromophore to the particle. This process has been observed for a number of attached fluorescent compounds, such as small dyes [9–12], conjugated polymers [13], semiconductor quantum dots [14] and large molecules such as fullerenes [15]. Energy transfer to the gold core leads to quenching of porphyrin fluorescence in porphyrin-functionalized gold nanoparticles [4]. The energy transfer in porphyrins attached to gold nanoparticles by a relatively short linker results in shortening of the fluorescence lifetime of porphyrins to ~50 ps, as measured by a single photon counting setup [16].

This study presents the use of two thioacetate linkers on porphyrins (Scheme 1). In addition, the use of two different positions of the linkers on the porphyrin core should change the orientation of porphyrins bound to gold nanoparticles. The preparation of porphyrin-functionalized nanoparticles is carried out via a mild ligand exchange route. The effect of the different positions of the linkers is reviewed by evaluating the packing density and fluorescence lifetimes of the two porphyrin-functionalized gold nanoparticles. The fluorescence lifetimes of porphyrin-functionalized gold nanoparticles are measured using an up-conversion setup, which is an accurate method for determining very short (<100 ps) lifetimes.

2. Experimental

2.1. General

Solvents of analytical grade were obtained from commercial sources. Oxalyl chloride (96%), potassium thioacetate (98%), tetraoctylammonium bromide (TOABr) (98%) and sodium borohydride ($NaBH_4$) (96%) were purchased from Fluka and bromopropionic acid (97%) and gold(III) chloride trihydrate (99.9%) from Aldrich.

* Corresponding author. Tel.: +358 40 1981124; fax: +358 3 31152108.
E-mail address: anne.kotiaho@tut.fi (A. Kotiaho).

1010-6030/$ – see front matter © 2010 Elsevier B.V. All rights reserved.
doi:10.1016/j.jphotochem.2010.04.005

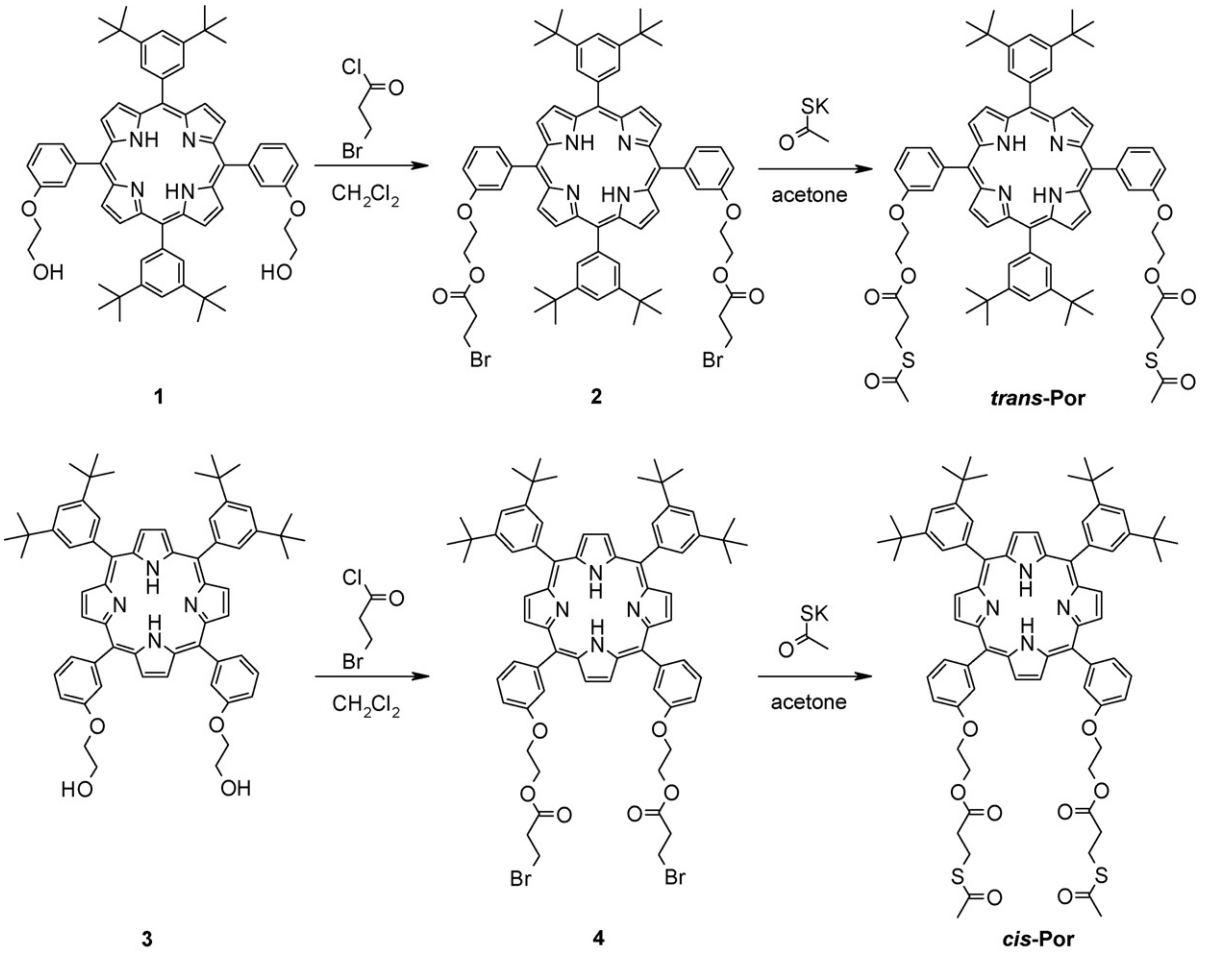

Scheme 1. Synthesis of porphyrins with thioacetate groups.

The ^{1}H NMR spectra were measured with a Varian Mercury 300 MHz spectrometer (Varian Inc.). All chemical shifts are given in ppm relative to TMS as internal standard. The mass spectra were recorded on ESI-TOF LCT Permier XE mass spectrometer (Waters Corp.). Original spectra were centered, and lock mass TOF correction was applied. The TEM analyses were carried out in an analytical transmission electron microscope (TEM), JEM 2010 from Jeol (Tokyo, Japan), operated at 200 kV.

2.2. Synthesis of thioacetate porphyrins

The synthetic steps for preparing *trans*-Por and *cis*-Por are shown in Scheme 1. Porphyrins with terminal OH-groups located on opposite or adjacent phenyl substituents of the porphyrin rings, 1 and 3, respectively, were synthesized as described earlier [17] and used as starting materials.

Typical procedure is as follows: porphyrin 1 or 3 was stirred with excess of 3-bromopropanoyl chloride in dichloromethane for 5–10 days. The crude product was washed exhaustively with water and purified on Silica 100 using chloroform as an eluent to yield porphyrin 2 or 4. Then, porphyrin 2 or 4 with terminal bromines was stirred overnight in acetone with excess of potassium thioacetate. The solvent was evaporated and the dry crude product was dissolved in chloroform and washed repeatedly with brine and water. Purification was done on Silica 60 using chloroform as an eluent. Yields of thioacetate porphyrins were 44% (*trans*-Por) and 88% (*cis*-Por) after the two reaction steps.

***trans*-Por**. ^{1}H NMR (300 MHz, $CDCl_3$) δ: 8.91–8.84 (m, 8H, β-*H*), 8.08 (d, J = 1.8 Hz, 4H, Ar-*H*), 7.85 (d, J = 7.4 Hz, 2H, Ar-*H*), 7.80 (t, J = 1.8 Hz, 2H, Ar-*H*), 7.79 (br s, 2H, Ar-*H*), 7.64 (t, J = 7.9 Hz, 2H, Ar-*H*), 7.36–7.30 (m, 2H, Ar-*H*), 4.53 (t, J = 4.7 Hz, 4H, OC_2H_4O), 4.35 (t, J = 4.7 Hz, 4H OC_2H_4O), 3.11 (t, J = 7.0 Hz, 4H, $COCH_2CH_2S$), 2.70 (t, J = 7.0 Hz, 4H, $COCH_2CH_2S$), 2.24 (s, 6H, $SCOCH_3$), 1.53 (s, 36H, $C(CH_3)_3$), −2.75 (s, 2H, N*H*).

ESI-TOF MS, in chloroform/methanol 1:1, m/z: found 1219.5638 ($M+H^+$), calcd. 1219.5652 for $C_{74}H_{83}N_4O_8S_2$.

***cis*-Por**. ^{1}H NMR (300 MHz, $CDCl_3$) δ: 8.92–8.84 (m, 8H, β-*H*), 8.07 (d, J = 1.5 Hz, 4H, Ar-*H*), 7.86 (d, J = 3.6 Hz, 2H, Ar-*H*), 7.80 (t, J = 1.8 Hz, 2H, Ar-*H*), 7.79 (br s, 2H, Ar-*H*), 7.65 (t, J = 7.9 Hz, 2H, Ar-*H*), 7.37-7.33 (m, 2H, Ar-*H*), 4.53 (t, J = 4.7 Hz, 4H, OC_2H_4O), 4.36 (t, J = 4.7 Hz, 4H, OC_2H_4O), 3.12 (t, J = 6.9 Hz, 4H, $COCH_2CH_2S$), 2.70 (t, J = 6.9 Hz, 4H, $COCH_2CH_2S$), 2.24 (s, 6H, $SCOCH_3$), 1.52 (s, 36H, $C(CH_3)_3$), −2.74 (s, 2H, N*H*).

ESI-TOF MS, in chloroform/methanol 1:1, m/z: found 1219.5721 ($M+H^+$), calcd. 1219.5652 for $C_{74}H_{83}N_4O_8S_2$.

2.3. Synthesis of gold nanoparticles (TOABr–AuNP)

A gold(III) chloride trihydrate aqueous solution (25 mM, 2 ml) was vigorously stirred with a toluene solution of TOABr (85 mM, 3 ml) until all of gold chloride was transferred to the organic phase. The reducing agent, $NaBH_4$, in an aqueous solution (36 mM, 2 ml) was added dropwise during 10 min. After addition of $NaBH_4$, the mixture was stirred vigorously for 20 min. The organic phase

was separated and washed with water. The obtained TOABr–AuNP toluene solution was used in a ligand exchange reaction.

2.4. Attachment of porphyrins to gold nanoparticles

The volume of TOABr–AuNP toluene solution (10 mg of gold) was evaporated to 1.5 ml and 2.0 mg of *cis*-Por or *trans*-Por was added. Approximated molar ratio of porphyrin-to-gold nanoparticle was 130. After 24 h of stirring, the reaction mixture was diluted with toluene and unreacted thioacetate porphyrins were separated in a size-exclusion column (Bio-Beads S-X3 from Bio-Rad) using toluene as an eluent.

2.5. Spectroscopic methods

Absorption spectra were measured with a Shimadzu UV-3600 UV–vis–NIR spectrophotometer. Steady-state fluorescence spectra were recorded with a Fluorolog 3 Yobin Yvon-SPEX spectrofluorometer. The emission spectra were corrected to instrument wavelength sensitivity using a correction spectrum supplied by the manufacturer.

Time-correlated single photon counting (TCSPC) system consisting of PicoHarp 300 controller and PDL 800-B driver (PicoQuant GmBH) was used for time-resolved fluorescence measurements on ns-timescale. Excitation wavelength was 405 nm from a pulsed diode laser head LDH-P-C-405B. Fluorescence signal was detected with a micro-channel plate photomultiplier (Hamamatsu R2809U). Time resolution was approximately 100 ps. Time-resolved fluorescence measurements on ps-timescale were done using up-conversion technique. The up-conversion measurement setup has been described in detail elsewhere [18].

3. Results and discussion

3.1. Synthesis and characterization

Synthetic scheme for preparing thioacetate porphyrins is shown in Scheme 1. 3-Bromopropanoyl chloride was prepared from oxalyl chloride and bromopropionic acid according to Ref. [19]. The synthesis of thioesters from halides has been described in detail in Ref. [20]. Thioacetate porphyrins were attached to pre-formed gold nanoparticles with a ligand exchange reaction. Method for preparing gold nanoparticles was similar to that described by Brust et al. [21], with a modification that the phase transfer agent TOABr serves also as the protecting ligand [22]. Sulphur binds to gold more strongly than TOABr and thus thioacetate porphyrins will exchange easily with TOABr.

Thioacetates adsorb to gold surfaces more slowly than thiols, but they can bind to gold surface in a similar way as thiols [23]. The different adsorption of thioacetates compared to thiols can lead to formation of less dense self-assembled monolayers on gold surfaces [24,25], or formation of bigger gold nanoparticles in the case of the Brust reaction [26]. Both thiols and thioacetates can form thiolate bond to the gold surface [5,6,24–26], but in the case of thioacetates adsorption of thioacetyl [27] or cleaved acetyl [28] group has also been observed.

The route used in preparation of porphyrin-functionalized gold nanoparticles is mild to the chromophore to be attached: it is not exposed to strong acidic or basic conditions due to gold precursor or reducing agent, respectively. Both of these possibly destructive steps are present in the classical Brust reaction. A drawback of the proposed method is the presence of TOABr in large amount, which can alter the properties of functionalized gold nanoparticles. On the other hand, TOABr can co-stabilize gold nanoparticles functionalized with big molecules, which sometimes suffer from instability and aggregation.

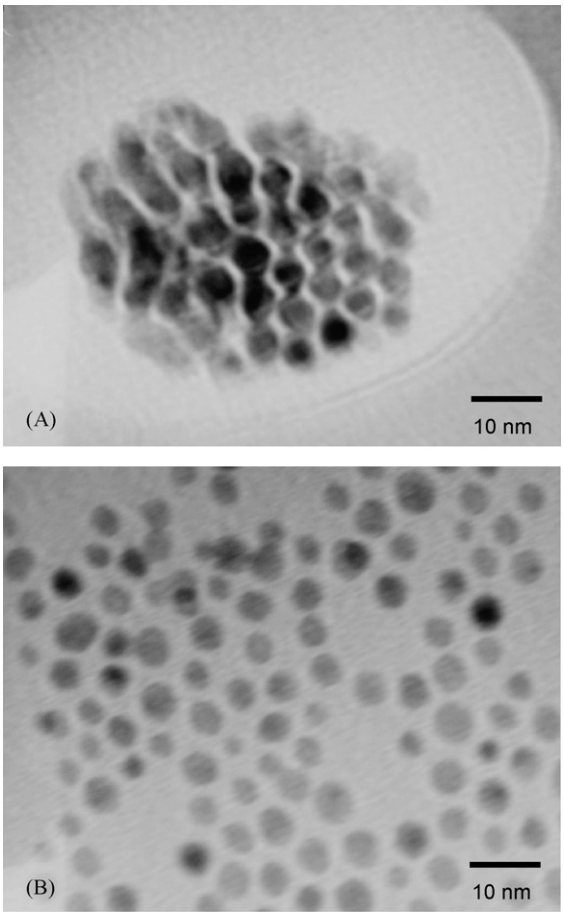

Fig. 1. TEM images of (A) TOABr–AuNP and (B) *cis*-Por-AuNP.

The NMR spectrum of *cis*-Por-AuNP (Supporting Information) shows intense peaks belonging to TOABr and weak peaks corresponding to porphyrin β- and Ar-protons. Importantly, the signal from the thioacetyl-protons has nearly disappeared for *cis*-Por-AuNP, indicating attachment of the porphyrins to the gold nanoparticles. The signals from the linker protons are less intense and broadened, which also indicates attachment to the gold nanoparticles, because the NMR signals of atoms close to gold nanoparticle surfaces are known to become broad or non-observable.

Both *cis*-Por-AuNP and *trans*-Por-AuNP were stable in toluene solutions obtained from ligand exchange reaction and purified with size-exclusion chromatography. *cis*-Por-AuNP could be dried and redissolved to a different solvent, whereas *trans*-Por-AuNP formed insoluble aggregates after the evaporation of toluene. Therefore NMR measurements of *trans*-Por-AuNP were not possible. The aggregation of *trans*-Por-AuNP can be caused either by insufficient protection of the gold nanoparticle surface by the porphyrins, or by unattached thioacetate linkers that connect particles together upon solvent evaporation. Also long-term stability of *trans*-Por-AuNP was poorer compared to *cis*-Por-AuNP, since the former slowly precipitates in toluene solution, whereas the toluene solutions of the latter are stable for months.

The core diameter of TOABr–AuNP was estimated from TEM images to be approximately 5 nm (Fig. 1A). The TEM images of *cis*-Por-AuNP show that the core diameter of the gold particles remains the same after modification with *cis*-Por. The packing of TOABr–AuNP (Fig. 1A) is pseudohexagonal with an interparticle distance comparable to the chain length of the protecting salt [22]. For *cis*-Por-AuNP, the interparticle distance is longer and packing

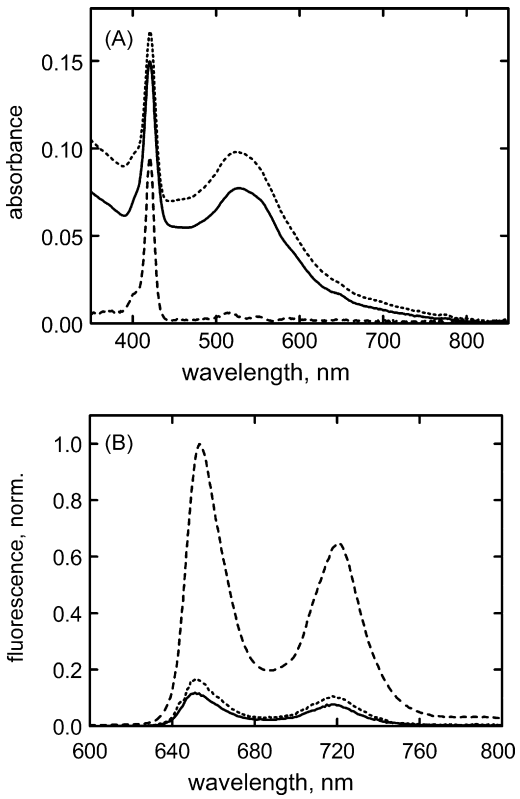

Fig. 2. (A) Absorption and (B) fluorescence spectra of *cis*-Por (dashed line), *cis*-Por-AuNP (solid line) and *trans*-Por-AuNP (dotted line). Both absorption and fluorescence of *trans*-Por are similar to *cis*-Por. Excitation wavelength in fluorescence measurements was 420 nm.

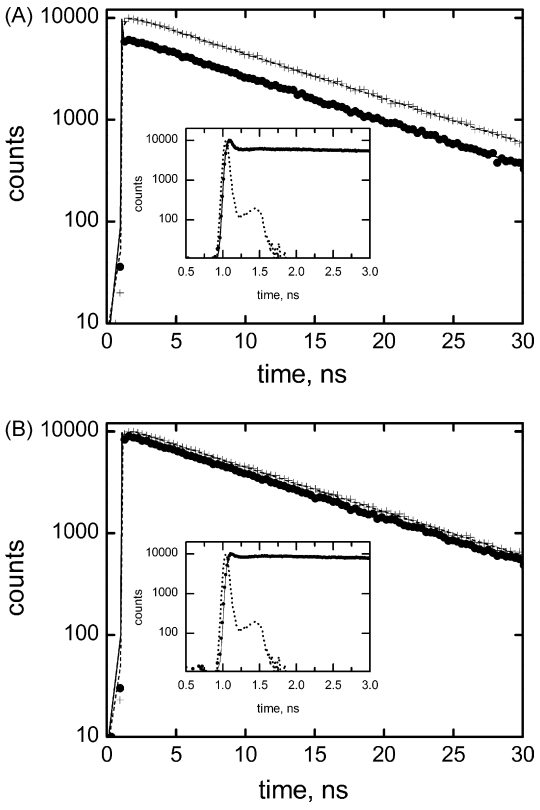

Fig. 3. Fluorescence decays from TCSPC with fits for (A) *cis*-Por (crosses and dashed line), *cis*-Por-AuNP (circles and solid line) and (B) *trans*-Por (crosses and dashed line) and *trans*-Por-AuNP (circles and solid line). Part of the data points is omitted for clarity. The insets show decays of porphyrin-functionalized gold nanoparticles on shorter time scales together with the instrument response function.

of the nanoparticles is almost random (Fig. 1B). The differences in the interparticle distance and packing are a good indication of porphyrins attaching to the surfaces of gold nanoparticles and forming a protecting layer.

3.2. Absorption and fluorescence spectra

Both *cis*-Por and *trans*-Por have Soret bands at 420 nm and the band red-shifts only 1 nm due the attachment to the AuNP surface (Fig. 2A). Surface plasmon absorption is observed around 526 nm in both the *cis*-Por-AuNP and *trans*-Por-AuNP. Absorption spectra were used in determining the porphyrin-to-gold nanoparticle ratio. Molar absorption coefficient of *cis*-Por and *trans*-Por is 480,000 M^{-1} cm^{-1}, and the same value is assumed for porphyrins, when attached to gold nanoparticles. Only porphyrins aligned parallel and very close to the gold nanoparticle surface show a change in the absorption coefficient [5]. Absorption coefficient for 5 nm gold nanoparticles is estimated to be ~15 ml mg^{-1} cm^{-1} at the maximum of surface plasmon band, using literature models for the dependence of the absorption coefficient on the core diameter [29,30]. The molar mass of the gold core can be estimated to be 758,000 g/mol, using calculated volume of the 5 nm gold nanoparticle sphere, ~65,400 $Å^3$, and volume of one gold atom, 17 $Å^3$ [31]. Molar absorption coefficients of TOABr–AuNP are thus 1.1×10^7 M^{-1} cm^{-1} at 526 nm and $\sim 0.7 \times 10^7$ M^{-1} cm^{-1} at 460 nm. Gold nanoparticle concentration is calculated from absorbance at 460 nm, because the porphyrin absorption coefficient is negligible at this wavelength. Porphyrin concentration was calculated from absorbance at 420 nm, taking into account the underlying absorption of the gold nanoparticles. The estimated porphyrin-to-gold nanoparticle ratio is 30 for *cis*-Por-AuNP and 23 for *trans*-Por-AuNP. These values are rough estimates because of the several approximations made.

Porphyrin absorbances were adjusted to be the same at the excitation wavelength of 420 nm in samples of porphyrin-functionalized gold nanoparticles and thioacetate porphyrins prepared for fluorescence measurements. The porphyrin fluorescence in *cis*-Por-AuNP and *trans*-Por-AuNP is quenched to less than 20% of the free porphyrin fluorescence (Fig. 2B). Possible effect of TOABr on porphyrin fluorescence was checked by mixing TOABr in thioacetate porphyrin toluene solution, but no quenching of the porphyrin fluorescence was observed. Quenching of porphyrin fluorescence due to energy transfer to gold nanoparticles has been reported [4,32]. The same process is proposed to take place in *cis*-Por-AuNP and *trans*-Por-AuNP. The quenching can be partly caused by the intermolecular interactions between the porphyrins. However, aggregation of porphyrins usually leads to a shift and broadening of the Soret band. There is a minor change in the Soret-band position and width of the *cis*-Por and *trans*-Por molecules after attachment to the gold nanoparticles, indicating that the porphyrins are not aggregated on the nanoparticle surface.

3.3. Fluorescence lifetimes

The fluorescence decays measured by TCSPC for the porphyrins and porphyrin-functionalized gold nanoparticles are shown in Fig. 3. The lifetimes obtained from mono- or two-exponential fits are shown in Table 1. The fluorescence decay curves of *cis*-Por-AuNP and *trans*-Por-AuNP are a combination of a very fast decay (lifetimes 40 and 20 ps, respectively), which are poorly resolved both in magnitude and in lifetime by the TCSPC instrument, and a slow decay with similar lifetime as the porphyrin molecules in toluene solu-

Table 1
Fluorescence lifetimes (τ_i) and pre-exponential factors (a_i) obtained from fits of decay curves measured with TCSPC instrument.

	τ_1 (ps)	a_1 (%)	τ_2 (ns)	a_2 (%)	χ^2
cis-Por			9.82 ± 0.05		1.09
trans-Por			9.89 ± 0.05		1.11
cis-Por-AuNP	40 ± 10	54	9.83 ± 0.06	46	1.05
trans-Por-AuNP	20 ± 10	24	9.86 ± 0.05	76	1.11

tion. The longer lifetimes of *cis*-Por-AuNP and *trans*-Por-AuNP could originate from free, residual porphyrins, which indicates partially deficient purification. In a study by Imahori et al. on porphyrins attached to gold nanoparticles by one linker, a longer fluorescence lifetime was assigned to differently packed porphyrins [4].

The long fluorescence lifetimes (~9.8 ns) observed for *cis*-Por-AuNP and *trans*-Por-AuNP support the idea that most of the fluorescence of these systems is due to the fluorescence of free, residual porphyrins. The amount of fluorescent porphyrins derived from steady-state fluorescence spectra is 11 and 16% for *cis*-Por-AuNP and *trans*-Por-AuNP, respectively. This leads to reduction of the actually attached number of porphyrins to ~26 and 19 for *cis*-Por-AuNP and *trans*-Por-AuNP, respectively, when all the attached porphyrins are assumed to show no fluorescence in the steady-state spectra. If the gold nanoparticles are simply treated as spheres with a diameter of 5 nm, a value of 7800 Å^2 is obtained for the surface area. This gives molecular areas of ~300 and ~410 Å^2 for *cis*-Por-AuNP and *trans*-Por-AuNP, respectively.

The mean molecular area of porphyrin, with four 3,5-di-*tert*-butylphenyl-groups, aligned parallel to the surface is ~290 Å^2 in Langmuir–Blodgett films [33]. Both *cis*-Por and *trans*-Por can thus have parallel orientation relative to the gold nanoparticle surface, or more likely, they are sparsely packed on the gold nanoparticle surface. Looking at the molecular structures, *trans*-Por molecules attached by both linkers will most likely lie almost parallel to the gold nanoparticle surface because of the bulky di-*tert*-butylphenyl-groups will occupy a space at a same distance from the gold nanoparticle surface as the porphyrin plane itself. The poor resolubility of *trans*-Por-AuNP indicates that some of the *trans*-Por molecules might be attached to the nanoparticles only by one linker, though the relatively high mean molecular area indicates binding by two linkers. *cis*-Por molecules can in principle have any orientation between perpendicular and parallel relative to the gold nanoparticle surface.

Fluorescence lifetimes measured on ns-timescale with the TCSPC method indicate fluorescence lifetimes shorter than ~100 ps for the porphyrin molecules attached to the gold nanoparticles. With the up-conversion method, lifetimes can be measured with a time resolution down to ~0.1 ps. The fluorescence decays from the up-conversion measurements for porphyrin-functionalized gold nanoparticles are shown in Fig. 4. Measurement of porphyrin solutions with the same up-conversion setup was not possible due to fast degradation of the sample. The other reference sample, TOABr–AuNP, has a sharp signal (not shown in Fig. 4) that decays to zero in ~1 ps. This signal has a very low amplitude compared to the porphyrin signal and can be neglected in the analysis of decay curves of *cis*-Por-AuNP and *trans*-Por-AuNP. The choice of fitting procedure for fluorescence decays from the up-conversion measurements (Fig. 4) was done based on the assumption that the porphyrin molecules are not all attached in identical manner to the gold nanoparticle surface. The small differences in distances and orientations of individual porphyrins relative to the gold nanoparticle surface will lead to variation of the fluorescence lifetimes of porphyrins. This justifies the use of a stretched-exponential model [34,35], $I(t) = \exp[-(t/\tau)^{\beta}]$, where τ is the fluorescence lifetime and β is the stretching parameter. The stretched-exponential model

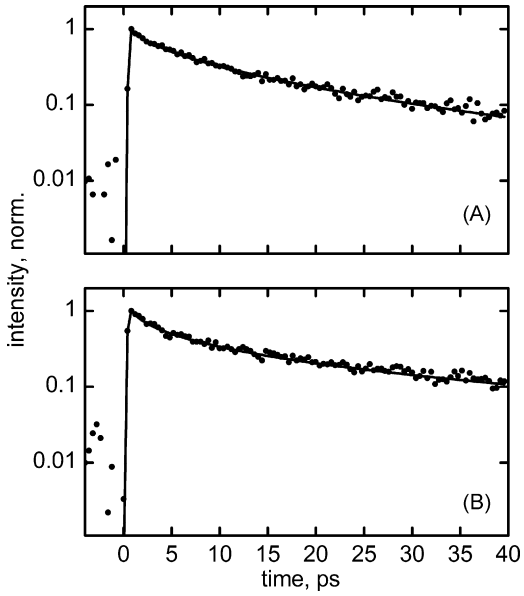

Fig. 4. Fluorescence decays and fits with stretched-exponential model for (A) *cis*-Por-AuNP and (B) *trans*-Por-AuNP. Excitation wavelength was 417 nm and monitoring wavelength was 660 nm.

can be used to describe heterogeneous systems. The magnitude of the parameter β is proportional to the variation of the system: the smaller the parameter is, the higher the diversity within the system is. The stretching parameter for *trans*-Por-AuNP is smaller than that for *cis*-Por-AuNP (Table 2), indicating more irregular attachment of *trans*-Por to the gold nanoparticle surface compared to *cis*-Por. The lifetime of *trans*-Por-AuNP is shorter than the lifetime of *cis*-Por-AuNP (Table 2).

The fluorescence lifetime of a chromophore attached to the surface of a gold nanoparticle of certain size depends essentially on two factors: the distance between the chromophore and the gold nanoparticle, and on the orientation of the chromophore relative to the gold nanoparticle surface [36]. Both of the porphyrin molecules studied here have flexible linkers, which complicates determination of the exact distance between the porphyrin core and gold nanoparticle surface. The linker length is roughly 1 nm [37]. Though the linkers used in the two porphyrin molecules have the same length, it does not mean that the actual distance between the porphyrin center and gold nanoparticle surface would be the same. It is reasonable to assume, based on the molecular structure obtained by simple modeling, that the distance between the porphyrin center and gold nanoparticle surface is shorter for *trans*-Por-AuNP. Metal nanoparticles can affect the rate of non-radiative decay of chromophores by adding relaxation pathway via energy transfer to the metal nanoparticle. At short (~1 nm) distance between a chromophore and the surface of gold nanoparticle, the probability for non-radiative decay is higher than that for the radiative decay [38]. Rate of energy transfer is only weakly dependent on the molecular orientation at short distances [39], with higher rate for perpendicular orientation compared to parallel orientation. As the energy transfer is distance dependent, the differences in fluorescence lifetimes of *cis*-Por-AuNP (more perpendicular) and *trans*-Por-AuNP

Table 2
Fluorescence lifetimes from up-conversion. τ is the fluorescence lifetime and β is the stretching parameter.

	β	τ (ps)	χ^2
cis-Por-AuNP	0.53 ± 0.03	5.4 ± 0.6	1.08
trans-Por-AuNP	0.39 ± 0.02	3.1 ± 0.6	1.04

(more parallel) can be explained better by the different distance of the molecules from the nanoparticle surface than by the differences in orientation.

Porphyrin-functionalized gold nanoparticles with a linker of 10–12 atoms between the porphyrin core and gold nanoparticle (core diameter ~2 nm) were reported to have a fluorescence lifetime of ~50 ps [16]. Lifetimes observed in the present report are significantly shorter, even though the linker is of similar length (11 atoms). Larger gold nanoparticles are more efficient energy acceptors than smaller ones [38], and this can partly explain the differences in the observed lifetimes. On the other hand, use of the up-conversion setup allows accurate determination of very short lifetimes.

4. Conclusions

Fluorescence lifetimes of porphyrin-functionalized gold nanoparticles were determined using the up-conversion method to be very short, 5.4 and 3.1 ps for *cis*-Por-AuNP and *trans*-Por-AuNP, respectively. The reduction of the porphyrin fluorescence lifetimes is ascribed to energy transfer to the gold core. The small differences in the fluorescence lifetimes and packing density of the two porphyrin molecules on the gold nanoparticle surface despite of the altered linker positions indicate that shorter or more rigid linkers are required for effective control of the orientation of the porphyrin molecules relative to the gold nanoparticle surface. Capping of gold cores with *cis*-Por molecules yields stable particles with covalently bound porphyrin molecules, whereas the *trans*-Por molecules are not as efficient in protecting the gold core against aggregation. The ligand exchange reaction using TOABr-protected gold nanoparticles and porphyrin thioacetates is applicable for attaching chemically sensitive molecules to gold nanoparticles because it avoids the harsh conditions of the traditional Brust method.

Acknowledgement

A.K. and R.L. acknowledge the Academy of Finland (No. 107182) for financial support.

Appendix A. Supplementary data

Supplementary data associated with this article can be found, in the online version, at doi:10.1016/j.jphotochem.2010.04.005.

References

[1] S. Yamada, T. Tasaki, T. Akiyama, N. Terasaki, S. Nitahara, Thin Solid Films 438–439 (2003) 70.
[2] S. Fukuzumi, Y. Endo, Y. Kashiwagi, Y. Araki, O. Ito, H. Imahori, J. Phys. Chem. B 107 (2003) 11979.
[3] P.D. Beer, D.P. Cormode, J.J. Davis, Chem. Commun. (2004) 414.
[4] H. Imahori, M. Arimura, T. Hanada, Y. Nishimura, I. Yamazaki, Y. Sakata, S. Fukuzumi, J. Am. Chem. Soc. 123 (2001) 335.
[5] M. Kanehara, H. Takahashi, T. Teranishi, Angew. Chem. Int. Ed. 47 (2008) 307.
[6] J. Ohyama, Y. Hitomi, Y. Higuchi, M. Shinagawa, H. Mukai, M. Kodera, K. Teramura, T. Shishido, T. Tanaka, Chem. Commun. (2008) 6300.
[7] S. Berner, H. Lidbaum, G. Ledung, J. Åhlund, K. Nilson, J. Schiessling, U. Gelius, J.-E. Bäckvall, C. Puglia, S. Oscarsson, Appl. Surf. Sci. 253 (2007) 7540.
[8] A.A. Yasseri, D. Syomin, V.M. Malinovskii, R.S. Loewe, J.S. Lindsey, F. Zaera, D.F. Bocian, J. Am. Chem. Soc. 126 (2004) 11944.
[9] A. Aguila, R.W. Murray, Langmuir 16 (2000) 5949.
[10] T. Gu, J.K. Whitesell, M.A. Fox, Chem. Mater. 15 (2003) 1358.
[11] T.L. Jennings, M.P. Singh, G.F. Strouse, J. Am. Chem. Soc. 128 (2006) 5462.
[12] T. Sen, S. Sadhu, A. Patra, Appl. Phys. Lett. 91 (2007) 043104.
[13] C. Fan, S. Wang, J.W. Hong, G.C. Bazan, K.W. Plaxco, A.J. Heeger, Proc. Natl. Acad. Sci. U.S.A. 100 (2003) 6297.
[14] T. Pons, I.L. Medintz, K.E. Sapsford, S. Higashiya, A.F. Grimes, D.S. English, H. Mattoussi, Nano Lett. 7 (2007) 3157.
[15] P.K. Sudeep, B.I. Ipe, K.G. Thomas, M.V. George, S. Barazzouk, S. Hotchandani, P.V. Kamat, Nano Lett. 2 (2002) 29.
[16] H. Imahori, Y. Kashiwagi, Y. Endo, T. Hanada, Y. Nishimura, I. Yamazaki, Y. Araki, O. Ito, S. Fukuzumi, Langmuir 20 (2004) 73.
[17] A. Efimov, P. Vainiotalo, N.V. Tkachenko, H. Lemmetyinen, J. Porphyrins Phthalocyan. 7 (2003) 610.
[18] N.V. Tkachenko, L. Rantala, A.Y. Tauber, J. Helaja, P.H. Hynninen, H. Lemmetyinen, J. Am. Chem. Soc. 121 (1999) 9378.
[19] M. Tercel, S.M. Stribbling, H. Sheppard, B.G. Siim, K. Wu, S.M. Pullen, K.J. Botting, W.R. Wilson, W.A. Denny, J. Med. Chem. 46 (2003) 2132.
[20] T.-C. Zheng, M. Burkart, D.E. Richardson, Tetrahedron Lett. 40 (1999) 603.
[21] M. Brust, M. Walker, D. Bethell, D.J. Schiffrin, R. Whyman, J. Chem. Soc., Chem. Commun. (1994) 801.
[22] J. Fink, C.J. Kiely, D. Bethell, D.J. Schiffrin, Chem. Mater. 10 (1998) 922.
[23] J.M. Tour, L. Jones II, D.L. Pearson, J.J.S. Lamba, T.P. Burgin, G.M. Whitesides, D.L. Allara, A.N. Parikh, S.V. Atre, J. Am. Chem. Soc. 117 (1995) 9529.
[24] M.I. Béthencourt, L. Srisombat, P. Chinwangso, T.R. Lee, Langmuir 25 (2009) 1265.
[25] M.G. Badin, A. Bashir, S. Krakert, T. Strunskus, A. Terfort, C. Wöll, Angew. Chem. Int. Ed. 46 (2007) 3762.
[26] S. Zhang, G. Leem, T.R. Lee, Langmuir 25 (2009) 13855.
[27] C.E. Inman, S.M. Reed, J.E. Hutchison, Langmuir 20 (2004) 9144.
[28] H. Skulason, C.D. Frisbie, J. Am. Chem. Soc. 122 (2000) 9750.
[29] X. Liu, M. Atwater, J. Wang, Q. Huon, Colloids Surf. B: Biointerfaces 58 (2007) 3.
[30] G.A. Rance, D.H. Marsh, A.N. Khlobystov, Chem. Phys. Lett. 460 (2008) 230.
[31] D.V. Leff, P.C. Ohara, J.R. Heath, W.M. Gelbart, J. Phys. Chem. 99 (1995) 7036.
[32] A. Kotiaho, R. Lahtinen, H. Lehtivuori, N.V. Tkachenko, H. Lemmetyinen, J. Phys. Chem. C 112 (2008) 10316.
[33] M. Anikin, N.V. Tkachenko, H. Lemmetyinen, Langmuir 13 (1997) 3002.
[34] M.N. Berberan-Santos, E.N. Bodunov, B. Valeur, Chem. Phys. 315 (2005) 171.
[35] R. Métivier, I. Leray, J.-P. Lefèvre, M. Roy-Auberger, N. Zanier-Szydlowski, B. Valeur, Phys. Chem. Chem. Phys. 5 (2003) 758.
[36] J. Gersten, A. Nitzan, J. Chem. Phys. 75 (1981) 1139.
[37] Calculated using ArgusLab 4.0.1, Mark A. Thompson, Planaria Software LLC, Seattle, WA, http://www.arguslab.com.
[38] S. Vukovic, S. Corni, B. Mennucci, J. Phys. Chem. C 113 (2009) 121.
[39] S. Bhowmick, S. Saini, V.B. Shenoy, B. Bagchi, J. Chem. Phys. 125 (2006) 181102.